

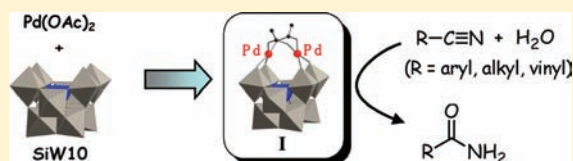
Palladium(II) Containing γ -Keggin Silicododecatungstate That Efficiently Catalyzes Hydration of Nitriles

Tomohisa Hirano, Kazuhiro Uehara, Keigo Kamata, and Noritaka Mizuno*

Department of Applied Chemistry, School of Engineering, The University of Tokyo, 7-3-1 Hongo, Bunkyo-ku, Tokyo 113-8656, Japan.

S Supporting Information

ABSTRACT: A mixture of $\text{Pd}(\text{OAc})_2$ and $\text{TBA}_4[\gamma\text{-SiW}_{10}\text{O}_{34}(\text{H}_2\text{O})_2]$ (TBA-SiW_{10} , $\text{TBA} = [(n\text{-C}_4\text{H}_9)_4\text{N}]^+$) showed high catalytic activities for hydration of various kinds of structurally diverse nitriles including aromatic, aliphatic, heteroaromatic, and double bond-containing ones. For hydration of 3-cyanopyridine, the turnover frequency was 860 h^{-1} , and the turnover number reached up to 670. A dipalladium-substituted γ -Keggin silicododecatungstate, $[\gamma\text{-H}_2\text{SiW}_{10}\text{O}_{36}\text{Pd}_2(\text{OAc})_2]^{4-}$ (**I**), was successfully synthesized by the reaction of $[\gamma\text{-SiW}_{10}\text{O}_{34}(\text{H}_2\text{O})_2]^{4-}$ with $\text{Pd}(\text{OAc})_2$ in a mixed solvent of acetone and water. The crystal structure of **I** was a monomeric, dipalladium-substituted, γ -Keggin silicododecatungstate with bidentate acetate ligands. Compound **I** showed similar activities and selectivities to those of a simple mixture of $\text{Pd}(\text{OAc})_2$ and TBA-SiW_{10} . The kinetic, mechanistic, and density functional theory calculation studies show that the dipalladium site plays an important role in the present hydration, and the nucleophilic attack of a hydroxide or water to the nitrile carbon atom is included in the rate-determining step.



INTRODUCTION

Hydration of nitriles to amides is one of the most important functional group transformations because amides have widely been utilized as chemical intermediates in organic synthesis as well as industrially important raw materials for lubricants, detergent additives, drug stabilizers, and functional polymers.¹ Classical hydration with H_2SO_4 and NaOH often produces undesirable carboxylic acids as byproducts. In addition, stoichiometric amounts of salts are formed in the workup (neutralization) step. To overcome these problems, various catalytic systems under neutral conditions have been developed.^{2–4} With regard to enzymatic hydration (including hydration with related model complexes), the reaction mechanism that involves cooperative activation of nitrile and water with two or more metallic centers has been proposed.^{5–7} While catalytic hydration by di- and multimetallic complexes (Mo , Ru , Ni , Pd , Rh , Os , and Au) has also been reported, these systems have disadvantages: (i) turnover frequencies (TOFs = $0.3\text{--}295 \text{ h}^{-1}$) are low,^{8,9} (ii) reaction rates for hydration of heteroaromatic nitriles are usually lower than those of common nitriles because of their strong coordination to the metal centers, and/or (iii) microwave irradiation or additives such as acids and bases are required to attain high yields of amides (Table S1).¹⁰

Polyoxometalates (POMs) are anionic metal–oxygen clusters of early transition metals and have a diverse range of application such as medicine, electrochemistry, material science, and catalysis because their chemical and physical properties can be finely tuned.^{11,12} Interests in catalysis by metal-substituted POMs have significantly grown because structures of the active sites can be designed at atomic and molecular levels. Especially, a lacunary γ -Keggin silicododecatungstate, $[\gamma\text{-SiW}_{10}\text{O}_{36}]^{8-}$, acts as

an inorganic ligand to construct di- and multimetallic active sites. We have recently reported that simply mixing metal salts and lacunary $[\gamma\text{-SiW}_{10}\text{O}_{36}]^{8-}$ under catalytic conditions leads to in situ formation of active catalysts.¹³ We apply such methodology to investigation of active catalysts for hydration of nitriles. In this contribution, we report efficient hydration of various kinds of structurally diverse nitriles including aromatic, aliphatic, heteroaromatic, and double bond-containing ones catalyzed by simply mixing $\text{Pd}(\text{OAc})_2$ and $\text{TBA}_4[\gamma\text{-SiW}_{10}\text{O}_{34}(\text{H}_2\text{O})_2]$ (TBA-SiW_{10} , $\text{TBA} = [(n\text{-C}_4\text{H}_9)_4\text{N}]^+$) and the catalyst isolation. The reaction mechanism is also investigated on the basis of kinetic, spectroscopic, and computational results.

RESULTS AND DISCUSSION

Effects of metal additives to TBA-SiW_{10} on hydration of benzonitrile (**1a**) to benzamide (**2a**) in *N,N*-dimethylformamide (DMF) were investigated (Table 1). Only $\text{Pd}(\text{OAc})_2$ dramatically accelerated the hydration without formation of benzoic acid (Table 1, entry 1, >99% yield of **2a**), while the other metal additives ($\text{Ni}(\text{OAc})_2$, $\text{Ag}(\text{OAc})$, $\text{Co}(\text{OAc})_2$, $\text{Cu}(\text{OAc})_2$, $\text{Rh}(\text{OAc})_2$, $\text{Zn}(\text{OAc})_2$, $\text{Mn}(\text{OAc})_2$, $\text{Fe}(\text{OAc})_2$, $\text{Pt}(\text{OAc})_2$, $[\text{Ru}_3(\mu_3\text{-O})(\text{OAc})_6(\text{H}_2\text{O})_3](\text{OAc})$, RuCl_3 , IrCl_3 , and RhCl_3) were less effective (<1–40% yields) (Table 1, entries 2–14). Each of $\text{Pd}(\text{OAc})_2$ and TBA-SiW_{10} and combination of $\text{Pd}(\text{OAc})_2$ with monovacant $[\alpha\text{-SiW}_{11}\text{O}_{39}]^{8-}$ or fully occupied $[\alpha\text{-SiW}_{12}\text{O}_{40}]^{4-}$ gave lower yields (Table 1, entries 15–18).¹⁴

The scope of the present $\text{Pd}(\text{OAc})_2\text{-TBA-SiW}_{10}$ system was examined (Table 2). Benzonitriles with electron-donating as well as -withdrawing substituents at different positions (**1b–1e**)

Received: January 25, 2012

Published: March 19, 2012

Table 1. Hydration of Benzonitrile (1a) to Benzamide (2a)^a

entry	catalyst	yield (%)
1	TBA-SiW10 + Pd(OAc) ₂	>99
2	TBA-SiW10 + Ni(OAc) ₂ ·4H ₂ O	9
3	TBA-SiW10 + Ag(OAc)	9
4	TBA-SiW10 + Co(OAc) ₂ ·4H ₂ O	<1
5	TBA-SiW10 + Cu(OAc) ₂ ·H ₂ O	2
6	TBA-SiW10 + Rh(OAc) ₂ ·H ₂ O	18
7	TBA-SiW10 + Zn(OAc) ₂ ·2H ₂ O	<1
8	TBA-SiW10 + Mn(OAc) ₂ ·4H ₂ O	<1
9	TBA-SiW10 + Fe(OAc) ₂	5
10	TBA-SiW10 + Pt(OAc) ₂ ·2AcOH	19
11	TBA-SiW10 + [Ru ₃ (μ ₃ -O)(OAc) ₆ (H ₂ O) ₃](OAc)	23
12	TBA-SiW10 + RuCl ₃	31
13	TBA-SiW10 + IrCl ₃	31
14	TBA-SiW10 + RhCl ₃	40
15 ^b	Pd(OAc) ₂	4
16 ^c	TBA-SiW10	10
17	TBA ₄ [α-SiW ₁₂ O ₄₀] + Pd(OAc) ₂	5
18	TBA ₄ [α-H ₄ SiW ₁₁ O ₃₉] + Pd(OAc) ₂	57
19 ^{c,d}	TBA-I	96
20 ^{c,e}	TPeA-I	94
21 ^{b,c,f}	AcOH	<1
22 ^{b,c}	without	<1

^aReaction conditions: POM (12.5 μmol), metal additive (metal: 25 μmol), **1a** (0.5 mmol), DMF (1.0 mL), water (10 mmol), 363 K, 9 h. Yield (%) = **2a** (mol)/initial **1a** (mol) × 100. Yields were determined by GC using naphthalene (10 mg) as an internal standard. ^bWithout POM. ^cWithout metal additive. ^dTBA-I (12.5 μmol). ^eTPeA-I (12.5 μmol). ^fAcOH (25 μmol).

could be converted into the corresponding amides (**2b–2e**) in high yields (Table 2, entries 3, 5, 7, and 9). Notably, hydration of *o*-methoxybenzonitrile (**1d**) gave **2d** in 88% yield.¹⁵ The present system showed high yields for hydration of easily coordinating 2-, 3-, and 4-cyanopyridines (**1f–1h**) (Table 2, entries 11, 15, and 17). For 15-mmol scale hydration of **1f**, 1.6 g of **2f** could be isolated (88% yield, 99% purity by ¹H NMR spectroscopy), showing that the present system is applicable to the gram-scale reaction (Table 2, entry 12). Nitriles containing heteroatoms such as oxygen and sulfur or 2-furancarboxitrile (**1i**) and 3-thiophenecarbonitrile (**1j**) were hydrated to the corresponding amides (**2i** and **2j**) in 90 and 75% yields, respectively (Table 2, entries 19 and 21). Less reactive aliphatic nitriles such as *n*-octanenitrile (**1k**) and acetonitrile (**1l**) were hydrated to afford the corresponding aliphatic amides (**2k** and **2l**) in excellent yields (Table 2, entries 23 and 25). Hydration of α,β-unsaturated nitrile, *trans*-cinnamonitrile (**1m**), proceeded only at the cyano group to afford the corresponding α,β-unsaturated amide (**2m**) in 89% yield (Table 2, entry 27). Industrially very important hydration of acrylonitrile (**1n**) also proceeded to give acrylamide (**2n**) (Table 2, entry 29). *To the best of our knowledge, efficient hydration by Pd-based catalysts applicable to a wide range of nitriles including nitrogen-containing heteroaromatic ones is unprecedented.*

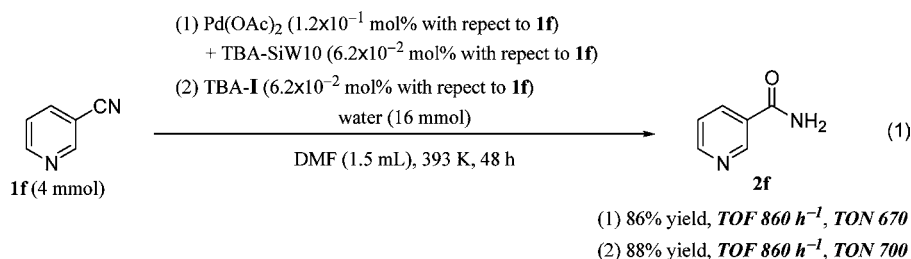
In order to further confirm the effectiveness of the present system, 4 mmol-scale hydration of **1f** was carried out. The hydration efficiently proceeded to give **2f** in 86% yield. The TOF was 860 h⁻¹ (determined by the initial rate based on Pd

Table 2. Hydration of Various Nitriles^a

Entry	Substrate	Product	Time (h)	Condition	Yield (%)
1					
2	1a	2a	9	A	>99
			9	B	96 (84)
3	1b	2b	12	A	81
4			12	B	>99 (90)
5	1c	2c	20	A	93
6			20	B	90 (86)
7	1d	2d	48	A	88
8			48	B	91 (83)
9	1e	2e	12	A	95
10			12	B	94 (92)
11 ^b	1f	2f	16	A	88
12 ^c			16	A	96 (88)
13 ^b			16	B	98
14 ^d			16	B	98
15 ^b	1g	2g	16	A	95
16 ^b			16	B	>99
17 ^b	1h	2h	48	A	73
18 ^b			48	B	91
19	1i	2i	5	A	90
20			5	B	94 (89)
21	1j	2j	18	A	75
22			18	B	72
23 ^e	1k	2k	30	A	98
24			30	B	90
25	1l	2l	12	A	>99
26			12	B	>99
27	1m	2m	18	A	89
28			18	B	91
29	1n	2n	30	A	60
30			30	B	66

^aReaction conditions for A: Pd(OAc)₂ (25 μmol), TBA-SiW10 (12.5 μmol), nitrile (0.5 mmol), DMF (1.0 mL), water (10 mmol), 363 K. Reaction conditions for B: TBA-I (12.5 μmol), nitrile (0.5 mmol), DMF (1 mL), water (10 mmol), 363 K. Yield (%) = **2** (mol)/initial **1** (mol) × 100. Yields were determined by GC using naphthalene (10 mg), chlorobenzene (10 mg), or biphenyl (10 mg) as an internal standard. The values in the parentheses are the isolated yields. ^bWater (2 mmol). ^cPd(OAc)₂ (750 μmol), TBA-SiW10 (375 μmol), nitrile (15 mmol), DMF (30 mL), water (300 mmol). ^dA recovered catalyst was used. The reaction conditions were the same as those of entry 13. ^eWater (1 mmol).

content) and the turnover number (TON) reached up to 670 (eq 1). The TOF was at least 10 times larger than those (0.02–80 h⁻¹) reported for the Pd-catalyzed hydration (Table S2). In addition, the TON was much higher than those reported for hydration of nitrogen-containing heteroaromatic nitriles ([IPr]Au(NTf₂)₂) (15, IPr = *N,N'*-bis(2,6-diisopropylphenyl)-imidazol-2-ylidene, NTf₂⁻ = bis(trifluoromethanesulfonyl)amide),^{15b} Rh^I catalyst (495),^{15a} [(dippe)Ni(μ-H)]₂ (355, dippe = 1,2-bis(diisopropylphosphino)ethane),^{16a} RuCl₂{κ¹(P)-3-Ph₂PC₆H₄CH₂NH^tBu}(η⁶-1,3,5-C₆H₃Me₃) (20),^{16b} [Ru(methylal)]₂(cod)]/2-diphenylphosphanyl-4-pyridyl(dimethyl)amine (21,



cod = 1,5-cyclooctadiene),^{16c} [Cp'₂Mo(μ-OH)₂MoCp'₂][OTs]₂ (31, Cp' = η⁵-CH₃C₅H₄, OTs⁻ = tosylate),^{16d} and {[(PCy₃)-(CO)RuH]₄(μ₄-O)(μ₃-OH)(μ₂-OH)} (98, Cy = cyclohexyl),^{16e} while the value was lower than those of [PtH(PMe₂OH)-(PMe₂O)₂H] (2256)^{8c} and hydroxyapatite-supported silver nanoparticles (11000, AgHAP) (Table S3).^{4b,17}

The reaction of TBA-SiW10 with 2 equiv of Pd(OAc)₂ in a mixed solvent of DMF and water followed by addition of diethyl ether gave a yellow precipitate. The cold-spray ionization mass (CSI-MS) spectrum of the yellow precipitate in 1,2-dichloroethane exhibited the most intense peak (centered at *m/z* = 3988) with isotopic distribution that agrees with the pattern calculated for TBA₅[H₂SiW₁₀O₃₆Pd₂(OAc)₂]⁺ (Figure S1). These results suggest that TBA-SiW10 reacts with Pd(OAc)₂ in a mixed solvent of DMF and water to form a novel dipalladium-substituted POM with acetate ligands. The analytically pure dipalladium-substituted γ-Keggin silicodecatungstate, [γ-H₂SiW₁₀O₃₆Pd₂(OAc)₂]⁴⁻ (**I**), was obtained by the reaction of TBA-SiW10 with 2 equiv of Pd(OAc)₂ in a mixed solvent of acetone and water. The elemental analysis data revealed that the molar ratio of TBA/Pd/Si/W was 4:2:1:10, respectively. The IR spectrum of TBA-I showed the bands at 1590 and 1424 cm⁻¹ assignable to the asymmetric and symmetric stretching vibrations of carboxylate groups, respectively. Coordination modes of acetate ligands can be distinguished by the Δ(*ν*_{asym}(COO⁻) - *ν*_{sym}(COO⁻)) values.¹⁸ The present Δ value was 166 cm⁻¹ and in the range of those (116–173 cm⁻¹) of Pd complexes with bridging bidentate acetate ligands. The CSI-MS spectrum of TBA-I in 1,2-dichloroethane also exhibited the most intense parent peak (centered at *m/z* = 3988) assignable to TBA₅[H₂SiW₁₀O₃₆Pd₂(OAc)₂]⁺ (Figure 1a).¹⁹ These results suggest that **I** is a dipalladium-substituted silicodecatungstate with bridging bidentate acetate ligands.^{20,21} A TPeA salt of **I** (TPeA-I, TPeA = [(*n*-C₅H₁₁)₄N]⁺) was also obtained by the reaction of TPeA₄[γ-SiW₁₀O₃₄(H₂O)₂] with 2 equiv of Pd(OAc)₂.²²

The single crystals of TPeA-I suitable for X-ray crystallographic analysis were successfully obtained by recrystallization of TPeA-I in 1,2-dichloroethane. The anion structure of TPeA-I is shown in Figure 2. The crystallographic data are summarized in Table 3.²³ Two Pd atoms were incorporated into the lacunary sites of [γ-SiW₁₀O₃₆]⁸⁻ and in a square-planar arrangement: Each Pd atom was coordinated to two oxygen atoms of [γ-SiW₁₀O₃₆]⁸⁻ and bridged with two bidentate acetate ligands.²⁴ The O–Pd–O angles (86.3(5)–92.2(6)°) were very close to 90°. The Pd–O bond lengths (1.960(12)–2.027(15) Å) were close to those (1.96(1)–2.12(2) Å) reported for Pd-substituted POMs and typical Pd complexes with square-planar coordination geometry.^{25,26} Four TPeA cations per **I** anion could be crystallographically assigned, in accord with the result of the elemental analysis. The bond valence sum (BVS) values of palladium (2.27–2.31), tungsten

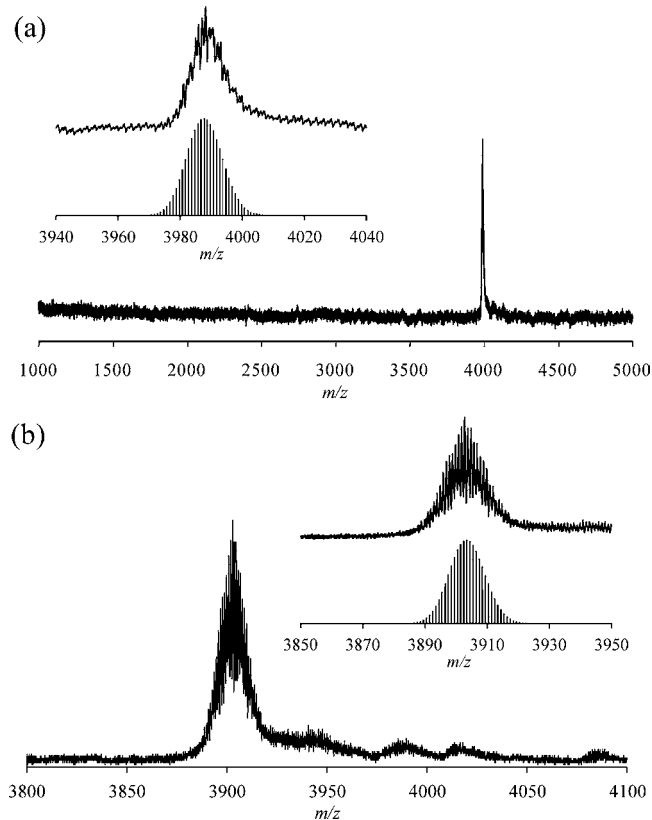


Figure 1. (a) Positive ion CSI-MS spectrum (*m/z* = 1000–5000) of TBA-I in 1,2-dichloroethane. Inset: Positive ion CSI-MS spectrum (*m/z* = 3940–4040) (top) and calculated patterns of TBA₅[H₂SiW₁₀O₃₆Pd₂(OAc)₂]⁺ (bottom). (b) Positive ion CSI-MS spectrum (*m/z* = 3800–4100) of TBA-I in acetone with 13500 equiv of water with respect to TBA-I. Inset: Positive ion CSI-MS spectrum (*m/z* = 3850–3950) (top) and calculated patterns of TBA₅[H₄SiW₁₀O₃₈Pd₂]⁺ (bottom).

(5.92–6.32), and silicon (4.04) indicate that respective valences are +2, +6, and +4. Therefore, two protons are associated with **I**. The BVS values of O3, O20, and O2 were 1.23, 1.48, and 1.54, respectively, and lower than those (1.70–2.10) of the other oxygen atoms, suggesting that O3 is monoprotonated and the other proton is disordered over O20 and O2.²³ The X-ray crystallographic, elemental analysis, and thermogravimetric data show that the formula of TPeA-I is TPeA₄[γ-H₂SiW₁₀O₃₆Pd₂(OAc)₂]. There are some examples of structurally characterized Pd-containing POMs, while most Pd atoms are sandwiched between two lacunary POMs and the four equatorial coordination sites are bound to POM frameworks.²⁵ To the best of our knowledge, this is the first example of the structurally characterized monomeric dipalladium-substituted

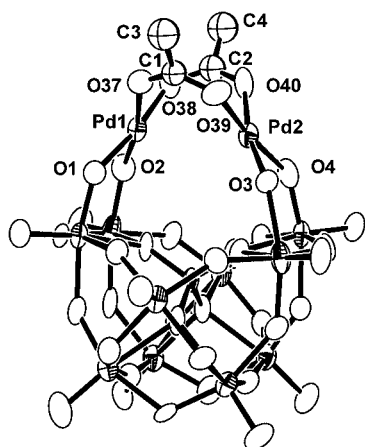
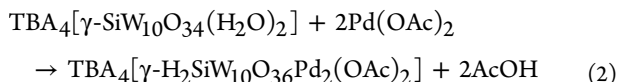


Figure 2. ORTEP drawing of the anion part of TPeA-I drawn at 50% probability level.

Table 3. Crystallographic Data for TPeA-I

TPeA-I	
formula	C ₁₆₈ N ₈ O ₈₀ Pd ₄ Si ₂ W ₂₀
fw	7571.54
crystal system	monoclinic
space group	P2/a (No. 13)
a (Å)	20.2918(2)
b (Å)	45.0388(4)
c (Å)	29.4768(3)
α (deg)	90.0000
β (deg)	89.94(0)
γ (deg)	90.0000
V (Å ³)	26939.4(5)
Z	4
gof	1.054
μ (mm ⁻¹)	8.831
no. of parameters refined	1822
R ₁ [I > 2σ(I)]	0.0924 (for 36825 data)
wR ₂	0.2303 (for all 64820 data)

γ-Keggin silicodcatungstate. The formation of TBA-I can be expressed by eq 2.



Hydration of **1a** to **2a** mediated by **I** was carried out under the reaction conditions in Table 1. The yields of **2a** with TBA-I and TPeA-I were 96 and 94%, respectively, and nearly the same (Table 1, entries 19 and 20).^{27,28} In addition, TBA-I showed similar reactivities to those of a mixture of Pd(OAc)₂ and TBA-SiW10 for various kinds of structurally diverse nitriles including aromatic, aliphatic, heteroaromatic, and double bond-containing ones (see the values under the conditions B in Table 2). For hydration of **1a**, the reaction rate (5.5 mM min⁻¹) of a mixture of Pd(OAc)₂ and TBA-SiW10 was almost the same as that (5.6 mM min⁻¹) of TBA-I.

The color of the reaction solution was yellow during hydration of **1f** with TBA-I, and no formation of palladium black was observed (Figure S3). After completion of hydration of **1f**, the catalyst could be recovered in an almost quantitative yield (93%) by addition of an excess amount of

1,2-dimethoxyethane to the reaction solution (precipitation method, see the Supporting Information). The palladium content in the filtrate was less than 0.5% of that in fresh **I**, indicating that the palladium species hardly leach into the reaction solution.²⁹ The recovered catalyst could be reused for hydration of **1f** without an appreciable loss of its high catalytic performance (Table 2, entries 13 and 14).³⁰

Upon addition of water to a DMF-*d*₇ solution of TBA-I at 363 K, the ¹H NMR signal at 1.62–1.65 ppm assignable to methyl protons of acetate ligands in **I** almost disappeared, and that at 1.96 ppm assignable to free acetic acid (1.5 ± 0.2 equiv with respect to **I**) appeared. Similarly, upon addition of water, the CSI-MS peak at *m/z* = 3988 assignable to TBA₅[H₂SiW₁₀O₃₆Pd₂(OAc)₂]⁺ of TBA-I almost disappeared, and the intense peak (centered at *m/z* = 3903) with isotopic distribution that agrees with the pattern calculated for TBA₅[H₄SiW₁₀O₃₈Pd₂]⁺ appeared (Figure 1b).³¹ These results suggest that the acetate ligands are eliminated by the reaction of **I** with water to form an acetate-free species (**II**). The Hammett plots (log(*k*_X/*k*_H) versus σ) for competitive hydration of **1a** and para-substituted benzonitriles are shown in Figure 3.

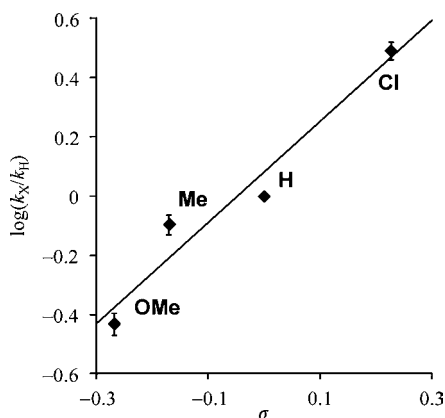


Figure 3. Hammett plots for competitive hydration of **1a** and para-substituted benzonitriles catalyzed by TBA-I. Reaction conditions: TBA-I (12.5 μmol), **1a** (0.25 mmol), para-substituted benzonitrile (0.25 mmol), water (10 mmol), DMF (1.0 mL), 363 K. Line fit: log(*k*_X/*k*_H) = 1.7109σ + 0.0813.

The positive ρ value (1.7) suggests formation of a negatively charged transition state. Similar positive ρ values have been reported for hydration catalyzed by AgHAP (ρ = 1.69) and a dinuclear molybdenum complex (ρ = 2.5), for which a nucleophilic attack of a hydroxide on the carbon atom of a coordinated nitrile has been proposed.^{4b,16d} The lower reaction rate of *o*-methoxybenzonitrile **1d** with respect to *p*-methoxybenzonitrile **1b** indicates a steric effect, suggesting coordination of a nitrile to the palladium center followed by nucleophilic attack of the hydroxide or water on the coordinated nitrile.^{4,15}

On the basis of these results and the kinetics provided below, we propose a possible reaction mechanism for the **I**-mediated hydration of nitriles. First, the acetate ligands are eliminated by the reaction of **I** with water to form **II** (eq 3). A nitrile reversibly coordinates to a palladium center in **II** and the complex with the coordinated nitrile (**III**) is formed (eq 4). Then, nucleophilic attack of the hydroxide or water on the nitrile carbon atom takes place to afford **II** and the corresponding amide (eq 5). The kinetic studies on the hydration of **1a** showed the first-order dependence of the reaction rate on

the concentration of **I** (5.2–15.6 mM, Figure 4a), and the saturation kinetics for the dependences of the reaction rates on

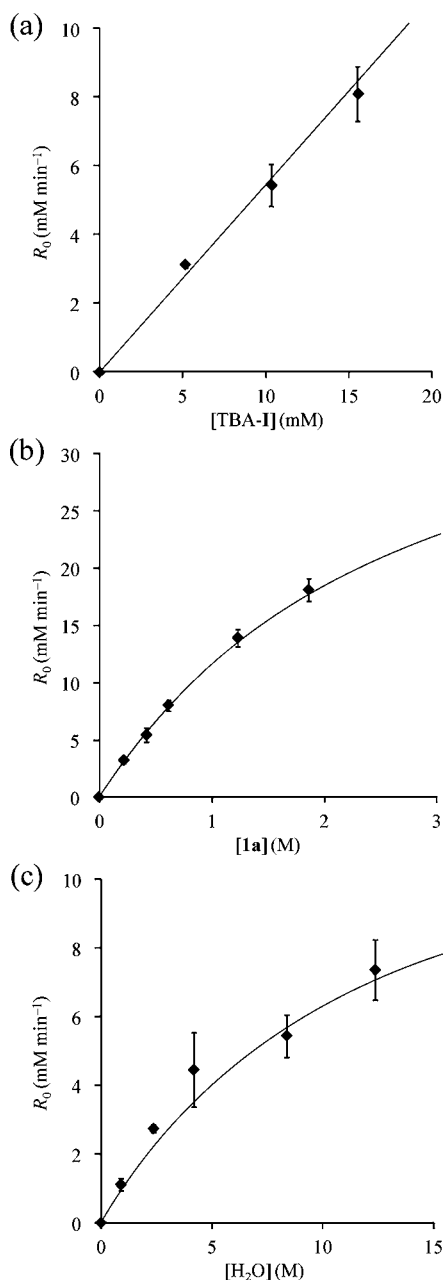
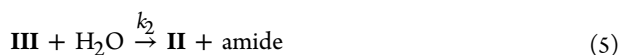


Figure 4. Dependence of the reaction rates on the concentration of (a) TBA-I, (b) **1a**, and (c) water. Reaction conditions for (a): TBA-I (5.2–15.6 mM), **1a** (0.42 M), water (8.3 M), DMF (1.0 mL), 363 K. Reaction conditions for (b): TBA-I (10.4 mM), **1a** (0.22–1.86 M), water (8.3 M), DMF (0.8–1.0 mL), 363 K. Reaction conditions for (c): TBA-I (10.4 mM), **1a** (0.42 M), water (0.9–12.4 M), DMF (0.8–1.1 mL), 363 K. Solid lines are simulation curves using eq 6.

the concentrations of **1a** (0.22–1.86 M, Figure 4b) and water (0.9–12.4 M, Figure 4c).



As mentioned above, the acetate ligands in **I** were almost completely eliminated by the reaction of **I** with water and were not observed in the recovered catalyst, showing that the concentration of **I** is almost zero. Therefore, the initial concentration of **I** ($[\mathbf{I}]_0$) is expressed by $[\mathbf{II}] + [\mathbf{III}]$. From the mass balance and steady-state approximation on **II**, the overall hydration rate is expressed by eq 6 (see details in Supporting Information).

$$R_0 = \frac{d[\text{amide}]}{dt} = \frac{k_1 k_2 [\mathbf{I}]_0 [\text{H}_2\text{O}] [\text{nitrile}]}{k_1 [\text{nitrile}] + k_2 [\text{H}_2\text{O}] + k_{-1}} \quad (6)$$

On the basis of the kinetic data, the k_1 , k_{-1} , and k_2 values were calculated to be $3.5 \pm 0.2 \text{ M}^{-1} \text{ s}^{-1}$, $5.6 \pm 0.4 \text{ s}^{-1}$, and $(5.4 \pm 0.1) \times 10^{-1} \text{ M}^{-1} \text{ s}^{-1}$, respectively. The dependences of the reaction rates on the concentrations of **I**, **1a**, and water calculated using eq 6 (shown by the solid lines in Figure 4) and the time course of hydration calculated by the numerical integration of eq 6 (shown by the solid lines in Figure S4) fairly well reproduced the experimental data.

The value for the kinetic isotope effect ($k_{\text{H}}/k_{\text{D}}$) was 0.9 ± 0.1 for the hydration of **1a** with water ($\text{H}_2\text{O}/\text{D}_2\text{O}$), suggesting that the O–H bond dissociation is not included in the rate-determining step. The good linearity of the Arrhenius plots was observed to afford the following activation parameters: $E_a = 78.3 \text{ kJ mol}^{-1}$, $\Delta H^\ddagger_{298 \text{ K}} = 75.3 \text{ kJ mol}^{-1}$, $\Delta S^\ddagger_{298 \text{ K}} = -15.7 \text{ J mol}^{-1} \text{ K}^{-1}$, $\Delta G^\ddagger_{298 \text{ K}} = 81.0 \text{ kJ mol}^{-1}$ (Figure 5). The present

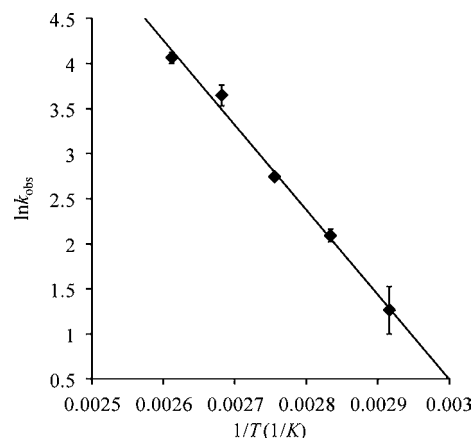


Figure 5. Arrhenius plots for hydration of **1a** catalyzed by TBA-I. The observed rate constants (k_{obs}) were determined from the initial part of the reactions. Reaction conditions: TBA-I (12.5 μmol , 10.4 mM), **1a** (0.5 mmol, 0.42 M), water (54 μL , 2.4 M), DMF (1.1 mL), 343–383 K. Line fit: $\ln k_{\text{obs}} = 28.76 - 9421.4/T$.

activation energy is much lower than that of hydration with H_2SO_4 ($E_a = 150.7 \text{ kJ mol}^{-1}$).³² The value of the activation entropy suggests that a bimolecular transition state is included in the rate-determining step.³³ All these results suggest that the nucleophilic attack of the hydroxide or water to the nitrile carbon atom is included in the rate-determining step under the present conditions.

In order to investigate the possible involvement of two palladium centers in catalyzing the present hydration, the density functional theory (DFT) calculations were carried out, taking into account the solvation in DMF using the conductor-like polarizable continuum model (IEFPCM) with the parameters of the United Atom Topological Model (UAHF). The transition-state structure and activation barrier for

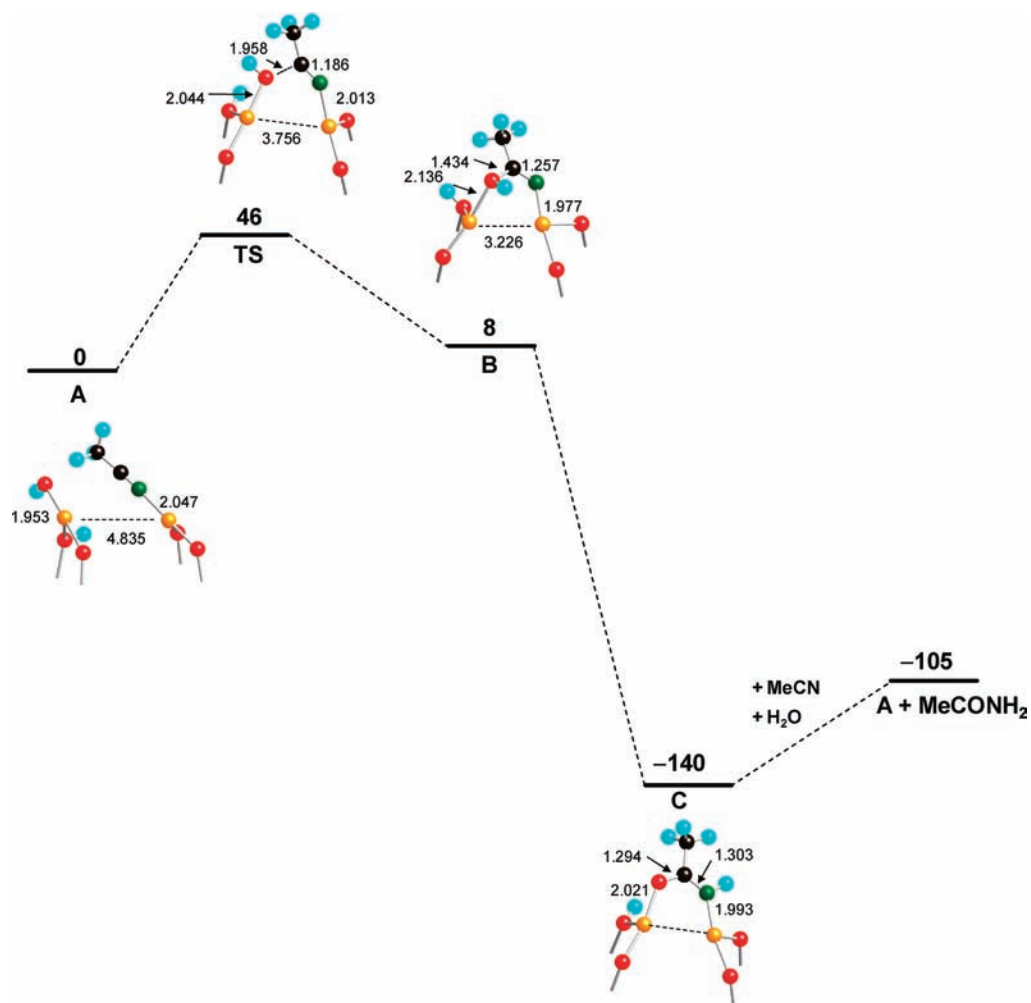


Figure 6. Calculated energy diagram of hydration of acetonitrile to acetamide on A (energies and lengths are in kJ mol^{-1} and \AA , respectively). Orange, red, black, green, and light-blue balls represent palladium, oxygen, carbon, nitrogen, and hydrogen atoms, respectively. Polyoxotungstate frameworks of $[\gamma\text{-SiW}_{10}\text{O}_{32}]$ are omitted for clarity.

hydration were calculated on the assumption that a starting model reactant was an acetate-free species with acetonitrile and hydroxide ion coordinated to each palladium center (A) (Figures 6 and S5). The intramolecular attack of the hydroxide to the nitrile carbon atom in A takes place to form the dipalladium iminolate species (B). This is the rate-determining step for the present hydration, and the activation barrier of the transition-state (TS) was calculated to be 46 kJ mol^{-1} . Then, intermediate B was converted into the dipalladium amidate species (C). Acetamide was eliminated through C followed by the reaction with acetonitrile and water, accomplishing the catalytic cycle. The computational results support that the dipalladium site plays an important role in the present hydration.

CONCLUSION

In summary, a mixture of $\text{Pd}(\text{OAc})_2$ and TBA-SiW10 showed high catalytic activities for hydration of various kinds of structurally diverse nitriles including aromatic, aliphatic, heteroaromatic, and double bond-containing ones. For hydration of **1f**, the TOF was 860 h^{-1} and the TON reached up to 670. A dipalladium-substituted γ -Keggin silicodetungstate, $[\gamma\text{-H}_2\text{SiW}_{10}\text{O}_{36}\text{Pd}_2(\text{OAc})_2]^{4-}$ (**I**), was successfully synthesized. The X-ray crystallographic analysis showed that **I**

had a monomeric structure, in which two Pd atoms were incorporated into the lacunary site of SiW10 and bridged with two bidentate acetate ligands. Compound TBA-I showed similar catalytic activities and selectivities to those of a simple mixture of $\text{Pd}(\text{OAc})_2$ and TBA-SiW10 for hydration of various kinds of nitriles. The kinetic, mechanistic, and theoretical studies show that the dipalladium site plays an important role in the present hydration and the nucleophilic attack of a hydroxide or water to the nitrile carbon atom is included in the rate-determining step. Cooperative activation of nitriles and water by the dipalladium site formed on a rigid POM framework leads to remarkable catalytic activity for hydration of nitriles.

EXPERIMENTAL SECTION

Materials. $\text{Pd}(\text{OAc})_2$ (Aldrich), tetra-*n*-butylammonium bromide (TCI), tetra-*n*-pentylammonium bromide (Acros Organics), acetone (Kanto Chemical), acetic acid (Kanto Chemical), diethyl ether (Kanto Chemical), 1,2-dichloroethane (Kanto Chemical), $\text{Na}_2\text{WO}_4 \cdot 2\text{H}_2\text{O}$ (Nippon Inorganic Color and Chemical), $\text{Na}_2\text{SiO}_3 \cdot 9\text{H}_2\text{O}$ (Wako Chemical), KCl (Nacalai Tesque), *N,N*-dimethylformamide (TCI), *N,N*-dimethylacetamide (Kanto Chemical), ethyl acetate (Kanto Chemical), *n*-hexane (Kanto Chemical), 1,2-dimethoxyethane (TCI), naphthalene (Wako Chemical), $\text{M}(\text{OAc})_x$ ($\text{M} = \text{Ag}, \text{Ni}$,

Co, Fe, Zn, Rh, Cu, and Mn) (TCI, Kanto Chemical, or Wako Chemical), $[\text{Ru}_3(\mu_3\text{-O})(\text{OAc})_6(\text{H}_2\text{O})_3](\text{OAc})$ (Tanaka Precious Metals), $\text{RuCl}_3 \cdot n\text{H}_2\text{O}$ (Wako Chemical), IrCl_3 (Aldrich), RhCl_3 (Aldrich), nitriles (TCI, Aldrich, or Kanto Chemical), and amides (TCI, Aldrich, or Wako Chemical) were purchased and used as received. Acrylonitrile (TCI) was purified according to the reported procedure.³⁴ The following compounds were synthesized according to literature procedures: $\text{Pt}(\text{OAc})_2 \cdot 2\text{AcOH}$,³⁵ $\text{K}_8[\gamma\text{-SiW}_{10}\text{O}_{36}] \cdot 12\text{H}_2\text{O}$,^{36,37} TBA-SiW_{10} ,^{36,37} and $\text{TPeA}_4[\gamma\text{-SiW}_{10}\text{O}_{36}(\text{H}_2\text{O})_2]$.^{36,37}

Instruments. IR spectra were measured on a Jasco FT/IR-460 Spectrometer Plus using KBr disks. NMR spectra were recorded on a JEOL ECA-500 spectrometer (^1H , 495.1 MHz; ^{13}C , 124.50 MHz; ^{29}Si , 98.37 MHz) by using 5 mm tubes. Chemical shifts (δ) were reported in ppm downfield from SiMe_4 (solvent, CDCl_3) for ^1H , ^{13}C , and ^{29}Si NMR spectra. CSI-MS spectra were recorded on a JEOL JMS-T100-CS spectrometer. Typical measurements were as follows: Orifice voltage 85 V for positive ions; sample flow 0.1 mL min^{-1} ; solvent 1,2-dichloroethane; concentration 0.1 mM; spray temperature 263 K; ion source at room temperature. X-ray diffraction measurements were made on a Rigaku AFC-10 Saturn 724 CCD detector with graphite monochromated $\text{Mo K}\alpha$ radiation ($\lambda = 0.71069 \text{ \AA}$). The data of TPeA-I were collected using CrystalClear³⁸ at 153 K, and indexing, integration, and absorption correction were performed with HKL2000³⁹ software for Linux. Neutral scattering factors were obtained from the standard source. In the data reduction, corrections for Lorentz and polarization effects were made. The structural analysis was performed using *CrystalStructure*⁴⁰ and Win-GX for Windows software.⁴¹ The molecular structure of TPeA-I was solved by combination of SHELXS-97 (direct methods) and SHELXH-97 (Fourier and least-squares refinement).⁴² Palladium, tungsten, silicon, and oxygen atoms were refined anisotropically, and carbon and nitrogen atoms were refined isotropically. The highly disordered solvent of crystallization (1,2-dichloroethane) was omitted by use of SQUEEZE program.⁴³ Detailed crystallographic data for TPeA-I are summarized in Table 3. Selected bond lengths and angles for TPeA-I are shown in Table S4. GC analyses were performed on Shimadzu GC-2014 with a flame ionization detector equipped with an InertCap 5 capillary column (internal diameter = 0.25 mm, length = 30 m), a TC-WAX capillary column (internal diameter = 0.25 mm, length = 30 m), or an RXi 5Sil MS capillary column (internal diameter = 0.25 mm, length = 60 m).

Synthesis and Characterization of $[(n\text{-C}_4\text{H}_9)_4\text{N}]_4[\gamma\text{-H}_2\text{SiW}_{10}\text{O}_{36}\text{Pd}_2(\text{OAc})_2]$ (TBA-I). Into a mixed solvent of acetone and water (4.88/0.12 mL), TBA-SiW10 (1.0 g, 293 μmol) was dissolved. To the solution were quickly added 2 equiv of $\text{Pd}(\text{OAc})_2$ (132 mg, 586 μmol), and the solution was stirred for 5 min at room temperature. Insoluble materials were removed by filtration, and the filtrate was stirred for 9 h at room temperature. The resulting yellow precipitates were collected by filtration and washed with acetone (1 mL) and diethyl ether (5 mL). After the precipitates were evacuated for 30 min at room temperature, the analytically pure TBA-I was obtained as yellow powders (449 mg, 41% yield). IR (KBr): 2961, 2935, 2873, 1590, 1484, 1424, 1383, 1153, 1089, 1015, 997, 954, 923, 876, 829, 779, 736, 561, 387, 363 cm^{-1} ; positive ion MS (CSI, 1,2-dichloroethane): m/z : 3988 $\text{TBA}_5[\text{H}_2\text{SiW}_{10}\text{O}_{36}\text{Pd}_2(\text{OAc})_2]^+$; ^1H NMR (495.1 MHz, 1,2-dichloroethane- d_4 , 298 K, SiMe_4) $\delta = 3.99\text{--}3.27$ (m), 1.77 (s), 1.71–1.65 (m), 1.52–1.46 (m), 1.00 (t, $J = 7.4$ Hz) ppm; ^{13}C {H} NMR (124.50 MHz,

1,2-dichloroethane- d_4 , 298 K, SiMe_4) $\delta = 187.0$, 58.7, 24.0, 22.9, 19.9, 13.7 ppm; ^{29}Si NMR (98.37 MHz, 1,2-dichloroethane- d_4 in the presence of four equivalents of AcOH with respect to TBA-I, 298 K, SiMe_4) $\delta = -83.9$ ($\Delta\nu_{1/2} = 4.4$ Hz); elemental analysis calcd (%) for $\text{C}_{68}\text{H}_{152}\text{N}_4\text{O}_{40}\text{Pd}_2\text{SiW}_{10}$ ($\text{TBA}_4[\text{H}_2\text{SiW}_{10}\text{O}_{36}\text{Pd}_2(\text{OAc})_2]$): C 21.81, H 4.09, N 1.50, Si 0.75, Pd 5.68, W 49.09; found: C 21.56, H 4.03, N 1.36, Si 0.75, Pd 5.77, W 49.23.

Synthesis and Characterization of $[(n\text{-C}_5\text{H}_{11})_4\text{N}]_4[\gamma\text{-H}_2\text{SiW}_{10}\text{O}_{36}\text{Pd}_2(\text{OAc})_2]$ (TPeA-I). Into a mixed solvent of acetone and water (1.95/0.05 mL) was dissolved TPeA- $[\gamma\text{-SiW}_{10}\text{O}_{36}(\text{H}_2\text{O})_2]$ (426 mg, 117 μmol). To the solution was quickly added $\text{Pd}(\text{OAc})_2$ (53 mg, 234 μmol), and the solution was stirred for 5 min at room temperature. Insoluble materials were removed by filtration, and the filtrate was stirred for 12 h at room temperature. Into the solution was added water (160 μL). After stirring the solution for 1 h, acetone (2 mL) was added, followed by addition of diethyl ether (3.6 mL). The solution was kept for one day at 278 K, and the yellow crystals of TPeA-I were obtained (273 mg, 59% yield). The single crystals suitable for X-ray crystallographic analysis were obtained by recrystallization of TPeA-I from 1,2-dichloroethane with addition of diethyl ether. IR (KBr): 2957, 2932, 2871, 1591, 1483, 1467, 1425, 1382, 1087, 1040, 1013, 996, 953, 922, 876, 827, 779, 735, 560, 443, 386, 363 cm^{-1} ; positive ion MS (CSI, 1,2-dichloroethane): m/z : 2282 $\text{TPeA}_6[\text{H}_2\text{SiW}_{10}\text{O}_{36}\text{Pd}_2(\text{OAc})_2]^{2+}$, 2946 $\text{TPeA}_{11}[\text{H}_2\text{SiW}_{10}\text{O}_{36}\text{Pd}_2(\text{OAc})_2]^{3+}$, 4267 $\text{TPeA}_5[\text{H}_2\text{SiW}_{10}\text{O}_{36}\text{Pd}_2(\text{OAc})_2]^+$; elemental analysis calcd (%) for $\text{C}_{84}\text{H}_{184}\text{N}_4\text{O}_{40}\text{Pd}_2\text{SiW}_{10}$ ($\text{TPeA}_4[\text{H}_2\text{SiW}_{10}\text{O}_{36}\text{Pd}_2(\text{OAc})_2]$): C 25.42, H 4.67, N 1.41, Si 0.71, Pd 5.36, W 46.31; found: C 25.23, H 4.80, N 1.35, Si 0.69, Pd 5.36, W 45.44.

General Procedure for Hydration of Nitriles. The catalytic hydration of nitriles was carried out in a 30-mL glass vessel containing a magnetic stir bar. A typical procedure for hydration of nitriles was as follows: Into a glass vessel were successively placed catalysts (conditions A in Table 2: $\text{Pd}(\text{OAc})_2$ (5.6 mg, 25 μmol) and TBA-SiW10 (42.8 mg, 12.5 μmol); conditions B in Table 2: TBA-I (46.8 mg, 12.5 μmol), naphthalene (10 mg), water (180 μL , 10 mmol), nitrile (0.5 mmol), and DMF (1.0 mL)). The reaction mixture was stirred at 363 K. The yields of the products were determined by the GC analysis using an internal standard technique. The isolation of amides was carried out by column chromatography on a silica gel (Silica Gel 60N, spherical, neutral, 63–210 μm , Kanto Chemical, cat. no. 37565–79) using *n*-hexane/ethyl acetate (5/5 \rightarrow 0/10 (v/v)) as an eluent.

Kinetic Studies. The reaction was carried out in a 15 mL glass vessel containing a magnetic stir bar. A typical procedure for kinetic studies was as follows: Into a glass vessel were successively placed naphthalene (10 mg), water (180 μL , 10 mmol), **1a** (0.5 mmol, 49.5 μL), and DMF (970 μL) (a total volume of water, **1a**, and DMF was 1.2 mL). Depending on the reaction conditions, the volume of DMF was changed to keep a total volume of water, **1a**, and DMF constant. After the solution was stirred for 12 min at 363 K, the reaction was initiated by addition of TBA-I (46.8 mg, 12.5 μmol). The reaction was periodically monitored by GC. Reaction rates (R_0) for the kinetic studies were determined from the slopes of reaction profiles (**[2a]** versus time) at low conversions (<20%) of **1a** (initial rate method).

Quantum Chemical Calculations. The DFT calculations were carried out at the B3LYP level theory⁴⁴ (6-31G(d,p) basis

sets for H, C, N, O, and Si atoms and the double- ξ quality basis sets with effective core potentials proposed by Hay and Wadt⁴⁵ for W and Pd atoms) by using conductor-like polarizable continuum model (IEFPCM) with the parameters of the United Atom Topological Model (UAHF). The entire structure of dipalladium-substituted POMs was used as a model. Acetonitrile was used as a model substrate. Transition-state structure was searched by numerically estimating the matrix of second-order energy derivatives at every optimization step and by requiring exactly one eigenvalue of this matrix to be negative. For the transition state, the frequency analysis was conducted at the same level at the final geometry. The optimized geometries were shown in Table S6 and Figure S5 (see the Supporting Information). The zero-point vibrational energies were not included. All calculations were performed with the Gaussian09 program package.⁴⁶

■ ASSOCIATED CONTENT

■ Supporting Information

Experimental details, CIF file of TPeA-I, Tables S1–S6, Figures S1–S6, and the complete citation of ref 46. This material is available free of charge via the Internet at <http://pubs.acs.org>.

■ AUTHOR INFORMATION

Corresponding Author

tmizuno@mail.ecc.u-tokyo.ac.jp

Notes

The authors declare no competing financial interest.

■ ACKNOWLEDGMENTS

We are grateful to Dr. K. Yamaguchi for fruitful discussions. This work was supported in part by the Japan Society for the Promotion of Science (JSPS) through its "Funding Program for World-Leading Innovative R&D on Science and Technology (FIRST Program), the Global COE Program (Chemistry Innovation through Cooperation of Science and Engineering), and a Grant-in-Aid for Scientific Research from the Ministry of Education, Culture, Science, Sports, and Technology of Japan. T.H. is grateful for a JSPS Research Fellowship for Young Scientists.

■ REFERENCES

- (1) Opsahl, R. In *Encyclopedia of Chemical Technology*; Kroschwitz, J. I., Ed.; Wiley: New York, 1992; pp 346–356.
- (2) Mascharak, P. K. *Coord. Chem. Rev.* **2002**, *225*, 201–214.
- (3) (a) Ahmed, T. J.; Knapp, S. M. M.; Tyler, D. R. *Coord. Chem. Rev.* **2011**, *255*, 949–974. (b) Kukushkin, V. Y.; Pombeiro, A. J. L. *Inorg. Chim. Acta* **2005**, *358*, 1–21.
- (4) (a) Yamaguchi, K.; Matsushita, M.; Mizuno, N. *Angew. Chem., Int. Ed.* **2004**, *43*, 1576–1580. (b) Mitsudome, T.; Mikami, Y.; Mori, H.; Arita, S.; Mizugaki, T.; Jitsukawa, K.; Kaneda, K. *Chem. Commun.* **2009**, 3258–3260.
- (5) Sträter, N.; Lipscomb, W. N.; Klabunde, T.; Krebs, B. *Angew. Chem., Int. Ed. Engl.* **1996**, *35*, 2024–2055.
- (6) (a) Steitz, T. A.; Steitz, J. A. *Proc. Natl. Acad. Sci. U.S.A.* **1993**, *90*, 6498–6502. (b) Meyer, F.; Kaifer, E.; Kircher, P.; Heinze, K.; Pritzkow, H. *Chem.–Eur. J.* **1999**, *5*, 1617–1630. (c) Bauer, C. B.; Concolino, T. E.; Eglin, J. L.; Rogers, R. D.; Staples, R. J. *J. Chem. Soc., Dalton Trans.* **1998**, 2813–2817.
- (7) The commonly accepted 'two metal-ion mechanism': One metal center enhances the electrophilicity of substrates, and the other metal facilitates the deprotonation of water to form a hydroxo species, leading to the intramolecular attack of the hydroxo species to the activated substrate.^{3b,6}
- (8) (a) Oshiki, T.; Yamashita, H.; Sawada, K.; Utsunomiya, M.; Takahashi, K.; Takai, K. *Organometallics* **2005**, *24*, 6287–6290. (b) García-Álvarez, R.; Díez, J.; Crochet, P.; Cadierno, V. *Organometallics* **2011**, *30*, 5442–5451. (c) Ghaffar, T.; Parkins, A. W. *J. Mol. Catal. A: Chem.* **2000**, *160*, 249–261.
- (9) There are only three reports on high TOFs (≥ 300 h⁻¹) of 20900 h⁻¹ (453 K),^{8a} 11400 h⁻¹ (373 K),^{8b} and 1485 h⁻¹ (363 K)^{8c} by monometallic complexes of *cis*-Ru(acac)₂(PPh₂Py)₂ (acac = acetylacetonato, PPh₂Py = diphenyl-2-pyridylphosphine), [RuCl₂(η^6 -C₆Me₆) {P(NMe₂)₃}], and [PtH(PMe₂OH)(PMe₂O)₂H], respectively.
- (10) While a dimetallic pathway is postulated for hydration of nitriles by dipalladium complexes with thiolate-hinged ligands, the system requires HBF₄ and applies to only two nitriles (acetonitrile and acrylonitrile): McKenzie, C. J.; Robson, R. *J. Chem. Soc., Chem. Commun.* **1988**, 112–114.
- (11) (a) Pope, M. T. *Heteropoly and Isopoly Oxometalates*; Springer-Verlag: Berlin, 1983. (b) Thematic issue on POMs. Hill, C. L. Ed.; *Chem. Rev.* **1998**, *98*, 1–390. (c) Pope, M. T. In *Comprehensive Coordination Chemistry II: Transition Metal Groups 3–6*; McCleverty, J. A.; Meyer, T. J., Eds.; Elsevier Science: New York, 2004; Vol. 4, pp 635–678. (d) Long, D.-L.; Tsunashima, R.; Cronin, L. *Angew. Chem., Int. Ed.* **2010**, *49*, 1736–1758.
- (12) (a) Hill, C. L.; Prosser-McCartha, C. M. *Coord. Chem. Rev.* **1995**, *143*, 407–455. (b) Okuhara, T.; Mizuno, N.; Misono, M. *Adv. Catal.* **1996**, *41*, 113–252. (c) Neumann, R. *Prog. Inorg. Chem.* **1998**, *47*, 310–370. (d) Kozhevnikov, I. V. *Catalysis by Polyoxometalates. In Catalysts for Fine Chemical Synthesis*; Wiley: Chichester, U.K., 2002; Vol. 2. (e) Mizuno, N.; Yamaguchi, K.; Kamata, K. In *Surface and Nanomolecular Catalysis*; Richards, R., Ed.; Taylor and Francis Group: New York, 2006; pp 463–491.
- (13) (a) Kikukawa, Y.; Yamaguchi, K.; Mizuno, N. *Angew. Chem., Int. Ed.* **2010**, *49*, 6096–6100. (b) Kikukawa, Y.; Kuroda, Y.; Yamaguchi, K.; Mizuno, N. *Angew. Chem., Int. Ed.* **2012**, *51*, 2434–2437.
- (14) The CSI-MS spectrum of a mixture of Pd(OAc)₂ and a monovacant POM TBA₄[α -H₄SiW₁₁O₃₉] in DMF exhibited the most intense peak (centered at *m/z* = 3995) with isotopic distribution that agrees with the pattern calculated for TBA₃[H₂SiW₁₁O₃₉Pd]⁺, showing formation of a monopalladium-substituted POM.
- (15) (a) Goto, A.; Endo, K.; Saito, S. *Angew. Chem., Int. Ed.* **2008**, *47*, 3607–3609. (b) Ramón, R. S.; Marion, N.; Nolan, S. P. *Chem.–Eur. J.* **2009**, *15*, 8695–8697.
- (16) (a) Crisóstomo, C.; Crestani, M. G.; García, J. J. *Inorg. Chim. Acta* **2010**, *363*, 1092–1096. (b) García-Álvarez, R.; Díez, J.; Crochet, P.; Cadierno, V. *Organometallics* **2010**, *29*, 3955–3965. (c) Muranaka, M.; Hyodo, I.; Okumura, W.; Oshiki, T. *Catal. Today* **2011**, *164*, 552–555. (d) Breno, K. L.; Pluth, M. D.; Tyler, D. R. *Organometallics* **2003**, *22*, 1203–1211. (e) Yi, C. S.; Zeczycki, T. N.; Lindeman, S. V. *Organometallics* **2008**, *27*, 2030–2035.
- (17) AgHAP shows high catalytic activity for hydration of aromatic nitriles, while the system is inactive for aliphatic ones. This high reactivity has been explained by the strong activation of aromatic nitriles on the silver nanoparticles through the dual activation of cyano and aromatic groups. The [PtH(PMe₂OH)(PMe₂O)₂H] system shows a wide substrate scope, and the cationic platinum species has been proposed to be active. For both systems, the rate laws have not been reported.
- (18) (a) Deacon, G. B.; Phillips, R. J. *Coord. Chem. Rev.* **1980**, *33*, 227–250. (b) Nakamoto, K. *Infrared Spectra of Inorganic and Coordination Compounds*; Wiley: New York, 1986.
- (19) The peaks assignable to TBA_{7-n}[H_nSiW₁₀O₃₆Pd₂(OAc)₂]⁺ (*n* = 0, 1, 3–7) were not observed for CSI-MS spectra of both a mixture of TBA-SiW10 with Pd(OAc)₂ and TBA-I. Therefore, the protonation state of the in situ prepared catalyst would be the same as that of isolated one.
- (20) Ion-pairing interactions (e.g., Na⁺...[P₂W₁₅Nb₃O₆₂]⁹⁻ ion-pairing) cause the appearance of extra signals or signal broadening for the solution NMR spectra.²¹ The ²⁹Si NMR spectrum of TBA-I in 1,2-dichloroethane showed one sharp signal at –83.9 ppm ($\Delta\nu_{1/2}$ = 4.4 Hz), and signal broadening due to the cation–POM ion-pairing

interactions was not observed. In addition, the peaks assignable to an ion-pair catalyst such as $\text{TBA}_4\{\text{Pd}(\text{OAc})\}[\text{H}_2\text{SiW}_{10}\text{O}_{36}\text{Pd}_2(\text{OAc})_2]^+$ were not observed for the CSI-MS spectrum of TBA-I in 1,2-dichloroethane. Therefore, an ion-pair catalyst such as $\{\text{Pd}(\text{OAc})^+ / [\text{H}_2\text{SiW}_{10}\text{O}_{36}\text{Pd}_2(\text{OAc})_2]^{4-}\}$ would not be formed. Detection of TBA-I by ^{183}W NMR spectroscopy was unsuccessful because the solubility of TBA-I in 1,2-dichloroethane was low, and the quantity was below the detection limit of ^{183}W nuclei.

(21) (a) Finke, R. G.; Lyon, D. K.; Nomiyama, K.; Sur, S.; Mizuno, N. *Inorg. Chem.* **1990**, *29*, 1784–1787. (b) Pohl, M.; Finke, R. G. *Organometallics* **1993**, *12*, 1451–1453.

(22) The elemental analysis data, IR spectrum, and CSI-MS spectrum of TPeA-I suggest that the anion structure is the same as that of TBA-I.

(23) The selected bond lengths and angles are summarized in Table S4. While there were two crystallographically independent anions (I_A and I_B) in the unit cell, these structures were almost identical with each other (see Figure S2). The structure of I_A is shown in Figure 2.

(24) Pope and co-workers reported a dichromium-substituted γ -Keggin silicodecatungstate with acetate ligands, $[\gamma\text{-SiW}_{10}\text{O}_{36}(\text{OH})\text{Cr}_2(\text{OAc})_2(\text{OH}_2)_2]^{5-}$; Wassermann, K.; Lunk, H.-J.; Palm, R.; Fuchs, J.; Steinfeldt, N.; Stösser, R.; Pope, M. T. *Inorg. Chem.* **1996**, *35*, 3273–3279.

(25) (a) Angus-Dunne, S. J.; Burns, R. C.; Craig, D. C.; Lawrance, G. A. *J. Chem. Soc., Chem. Commun.* **1994**, 523–524. (b) Bi, L.-H.; Reicke, M.; Körtz, U.; Keita, B.; Nadjo, L.; Clark, R. J. *Inorg. Chem.* **2004**, *43*, 3915–3920. (c) Bi, L.-H.; Körtz, U.; Keita, B.; Nadjo, L.; Borrmann, H. *Inorg. Chem.* **2004**, *43*, 8367–8372. (d) Bi, L.-H.; Körtz, U.; Keita, B.; Nadjo, L.; Daniels, L. *Eur. J. Inorg. Chem.* **2005**, 3034–3041. (e) Anderson, T. M.; Cao, R.; Slonkina, E.; Hedman, B.; Hodgson, K. O.; Hardcastle, K. I.; Neiwert, W. A.; Wu, S.; Kirk, M. L.; Knottenbelt, S.; Depperman, E. C.; Keita, B.; Nadjo, L.; Musaev, D. G.; Morokuma, K.; Hill, C. L. *J. Am. Chem. Soc.* **2005**, *127*, 11948–11949. (f) Anderson, T. M.; Cao, R.; Slonkina, E.; Hedman, B.; Hodgson, K. O.; Hardcastle, K. I.; Neiwert, W. A.; Wu, S.; Kirk, M. L.; Knottenbelt, S.; Depperman, E. C.; Keita, B.; Nadjo, L.; Musaev, D. G.; Morokuma, K.; Hill, C. L. *J. Am. Chem. Soc.* **2008**, *130*, 2877. (g) Villanneau, R.; Renaudineau, S.; Herson, P.; Boubekeur, K.; Thouvenot, R.; Proust, A. *Eur. J. Inorg. Chem.* **2009**, 479–488. (h) Bi, L.-H.; Dickman, M. H.; Körtz, U. *CrystEngComm* **2009**, *11*, 965–966. (i) Angus-Dunne, S.; Burns, R. C.; Craig, D. C.; Lawrance, G. A. *Z. Anorg. Allg. Chem.* **2010**, *636*, 727–734. (j) Izarova, N. V.; Banerjee, A.; Körtz, U. *Inorg. Chem.* **2011**, *50*, 10379–10386.

(26) (a) Bakhmutov, V. I.; Berry, J. F.; Cotton, F. A.; Ibragimov, S.; Murillo, C. A. *Dalton Trans.* **2005**, 1989–1992. (b) Kozitsyna, N. Y.; Nefedov, S. E.; Dolgushin, F. M.; Cherkashina, N. V.; Vargaftik, M. N.; Moiseev, I. I. *Inorg. Chim. Acta* **2006**, *359*, 2072–2086. (c) Nefedov, S. E.; Kozitsyna, N. Y.; Vargaftik, M. N.; Moiseev, I. I. *Polyhedron* **2009**, *28*, 172–180.

(27) The supported ruthenium hydroxide catalyst, $\text{Ru}(\text{OH})_x/\text{Al}_2\text{O}_3$ (Ru: 5 mol% with respect to **1a**), was almost inactive under the present reaction conditions in Table 1. In addition, heterogeneous nitrile hydration catalyzed by $\text{Ru}(\text{OH})_x/\text{Al}_2\text{O}_3$ requires a large amount of water (used as a solvent) and relatively high temperature (>403 K) to attain high yields of the corresponding amides.^{4a}

(28) DMF and *N,N*-dimethylacetamide were effective solvents for hydration of **1a** (Table S5); the I-mediated hydration in DMF and *N,N*-dimethylacetamide selectively gave **2a** without formation of benzoic acid, while water, dimethyl sulfoxide, and acetone gave **2a** in 48, 43, and 38% yields, respectively.

(29) After the recovery of catalyst, 1,2-dimethoxyethane was removed by evaporation, and **1f**, DMF, and water were added again. The solution was heated at 363 K for 16 h, and no reaction proceeded. These results ruled out leached palladium species from contributing to the catalysis.

(30) The ^1H NMR and IR spectra of the recovered catalyst showed the presence of **2f** and the absence of acetate ligands. The elemental analysis of the recovered catalyst revealed that the molar ratio of Pd:Si:W:**2f** was 2:1:10:4, respectively. The UV–vis spectrum of the recovered catalyst approximately agreed with the sum of these of

TBA-I(**2f**)₄, suggesting that the γ -Keggin structure of **I** is retained after the hydration.

(31) The CSI-MS spectrum of TBA-I in acetone upon addition of D_2O exhibited the most intense peak (centered at $m/z = 3903 + 4$) with isotopic distribution that agrees with the pattern calculated for $\text{TBA}_3[\text{D}_4\text{SiW}_{10}\text{O}_{38}\text{Pd}_2]^+$, supporting the elimination of the acetate ligands by the reaction with water.

(32) Sugiyama, K.; Miura, H.; Nakano, Y.; Sekiwa, H.; Matsuda, T. *Bull. Chem. Soc. Jpn.* **1986**, *59*, 2983–2989.

(33) (a) Pinnell, D.; Wright, G. B.; Jordan, R. B. *J. Am. Chem. Soc.* **1972**, *94*, 6104–6106. (b) Balahura, R. J.; Cock, P.; Purcell, W. L. *J. Am. Chem. Soc.* **1974**, *96*, 2739–2742. (c) Swartz, R. D.; Coggins, M. K.; Kaminsky, W.; Kovacs, J. A. *J. Am. Chem. Soc.* **2011**, *133*, 3954–3963.

(34) Perrin, D. D.; Armaego, W. L. F., Eds. *Purification of Laboratory Chemicals*, 3rd ed.; Pergamon Press: Oxford, 1988.

(35) Basato, M.; Biffis, A.; Martinati, G.; Tubaro, C.; Venzo, A.; Ganis, P.; Benetollo, F. *Inorg. Chim. Acta* **2003**, *355*, 399–403.

(36) Kamata, K.; Yonehara, K.; Sumida, Y.; Yamaguchi, K.; Hikichi, S.; Mizuno, N. *Science* **2003**, *300*, 964–966.

(37) Mizuno, N.; Uchida, S.; Kamata, K.; Ishimoto, R.; Nojima, S.; Yonehara, K.; Sumida, Y. *Angew. Chem., Int. Ed.* **2010**, *49*, 9972–9976.

(38) (a) *CrystalClear*, 1.4.0; Rigaku and Rigaku/MS: The Woodlands, TX, 1999. (b) Pflugrath, J. W. *Acta Crystallogr.* **1999**, *D55*, 1718–1725.

(39) Otwinowski, Z.; Minor, W. Processing of X-ray Diffraction Data Collected in Oscillation Mode. In *Methods of Enzymology*; Carter, C. W. Jr., Sweet, R. M., Eds.; Macromolecular Crystallography, Part A; Academic Press: New York, 1997; Vol. 276, pp 307–326.

(40) *CrystalStructure* 4.0; Rigaku and Rigaku/MS: The Woodlands, TX, 2000.

(41) Farrugia, L. J. *J. Appl. Crystallogr.* **1999**, *32*, 837–838.

(42) Sheldrick, G. M. *SHELX97, Programs for Crystal Structure Analysis*, Release 97-2; University of Göttingen: Göttingen, Germany, 1997.

(43) van der Sluis, P.; Spek, L. A. *Acta Crystallogr.* **1990**, *A46*, 194–201.

(44) Becke, A. D. *J. Chem. Phys.* **1993**, *98*, 1372–1377.

(45) Hay, P. J.; Wadt, W. R. *J. Chem. Phys.* **1985**, *82*, 270–283.

(46) Frisch, M. J. et al., *Gaussian 09*; Gaussian, Inc.: Wallingford, CT, 2009. See Supporting Information for the complete reference.